A CONCEPT FOR REDUCING PM_{10} EMISSIONS FOR CAR BRAKES BY 50%

[1]Perricone, Guido; [1]Matějka, Vlastimil; [1]Alemani, Mattia; [1]Valota, Giorgio; [1]Bonfanti, Andrea; [1]Ciotti, Alessandro; [2]Olofsson, Ulf; [2]Söderberg, Anders; [2]Wahlström, Jens; [2]Nosko, Oleksii; [3*]Straffelini, Giovanni; [3]Gialanella, Stefano; [3]Ibrahim, Metinoz.

[1] Brembo S.p.A., Bergamo, Italy
[2] Dept. of Machine Design, KTH Royal Institute of Technology, Stockholm, Sweden.
[3] Dept. of Industrial Engineering, University of Trento, Trento, Italy

*: *Corresponding Author*

KEYWORDS – Brakes, non-exhaust emissions, airborne particles, simulation, pin-on-disc test, dynamometer test.

ABSTRACT

With regard to airborne particles with an aerodynamic diameter of less than 10 μm (PM_{10}), in countries in the European Union, the mass of brake emissions equals approximately 8-27% of the total traffic-related emissions. Using a research methodology combining tests at different scale levels with contact mechanics simulations and PM_{10} chemical characterization, the REBRAKE EU-financed project had the following aims: i) to demonstrate the possibility of reducing the PM_{10} fraction of the airborne particulate from brake wear by 50 wt.%; ii) to enhance the general understanding on the physical and chemical phenomena underlying the brake wear process. The results achieved so far indicate that it is possible to design a disc brake system for a European standard car affording at least a 32 wt.% PM_{10} emission reduction using a standard European pad and a heat-treated rotor. A further reduction to 65 wt. % PM_{10} emission could be achieved with NAO pad material and the same heat-treated disc.

INTRODUCTION

Particles generated by road traffic originate not only from engine exhaust emissions, but also from wear processes occurring in brakes as well as between tyres and the road surface. In particular, a vehicle disc brake consists of a rotor and pads that are pressed against each other in order to reduce the vehicle speed by the friction drag generated at the contact interfaces. During the braking event, the friction pair wear out generating particles: the airborne fraction can penetrate the human body in many ways, including contact with the skin, breathing, and eating with potential adverse health effects [1]. The concentration of particulate matter (PM) continued to exceed the EU limit and target value in large parts of Europe in 2014 for which a total of 16% and 8% of the EU urban population was exposed respectively to PM_{10} and $PM_{2.5}$ (PM fraction consisting of particles with aerodynamic diameter of less than 10 μm and 2.5 μm respectively) levels above the daily limit value; considering the stricter WHO AQG values, the fraction of population affected changes to 50% and 85% respectively for PM_{10} and $PM_{2.5}$ [2]. Whilst exhaust gases from road transport are monitored and regulated by European legislation, little interest has been shown so far in PM originating from the wear of brakes, tyres and other non-exhaust emissions that altogether may amount to 50% by mass of the total ones [3], [4] and its relative contribution is expected to increase due to the legislation driven reduction of aerosols from vehicle combustion processes [5]. According to recent investigations [6], 16-55% by mass of non-exhaust emissions are generated by brake wear, and it was estimated that 50% of the

brake wear particles become airborne, 80-98% of which are in the PM_{10} range [7], [8]. Therefore, the reduction of airborne particles required to meet the EU objectives [9] could comprise a reduction in emissions from automobile brake wear.

Several studies can be found in the scientific literature concerning the relationship existing between wear mechanisms in disc brakes and relevant emissions of airborne PM [10], [11], [12], [13], [14], [15], [16], [17], [18], [19], [20], but all these studies have focused on commercial friction material without proposing a meaningful material optimization strategy to fix the brake wear particle emission issue. Friction material has also been studied in order to improve the understanding of health and environment issues [10], [21], [22], [23], [24],. To our knowledge, all these aspects have been studied separately without exploiting the synergic effects that could came from a holistic research approach.

In this framework, the main aim of the EU-FP7 REBRAKE project was to develop new materials for disc brakes, capable of reducing the amount of brake emitted PM_{10} for a standard European car by at least 50%. This main goal can be achieved through a holistic approach that includes: i) the tribological testing of the friction pair both at the system level and at the material level; ii) an analysis of the relevant wear products and correlated wear mechanisms, iii) the development of specific modelling approaches; iv) the optimization of the friction pair materials. Therefore, REBRAKE is also increasing a deeper comprehension of the physical and chemical phenomena underlying the brake wear process, including higher comprehension and analysis of characteristics coarse, fine and UFP particles.

In this overview, the main results obtained in the research are summarized, including future actions and development perspectives, which, thanks to the results achieved so far, have been contemplated and are regarded as being very promising with regard to reducing further brake emissions.

RESEARCH IMPLEMENTATION

A summary lay-out of the project is shown in Overview of the REBRAKE project.

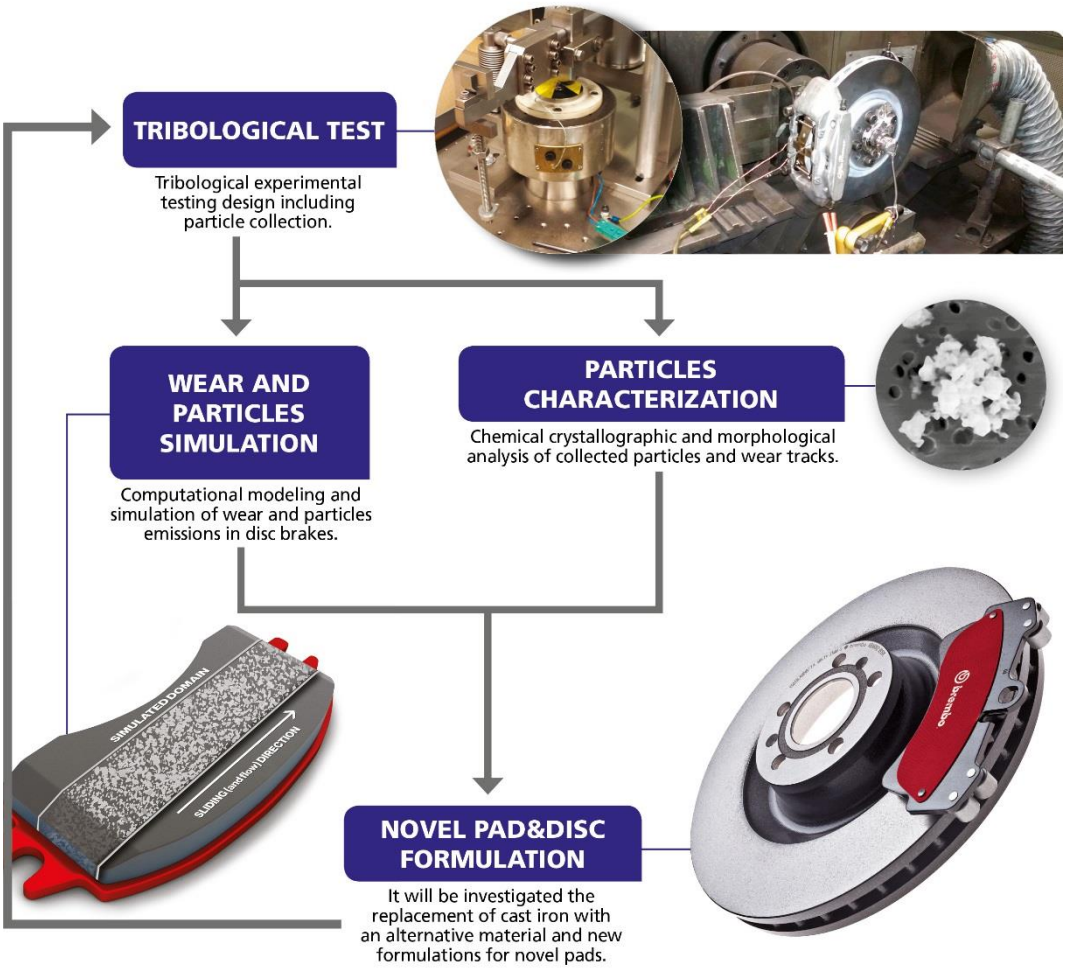

Fig. *1*

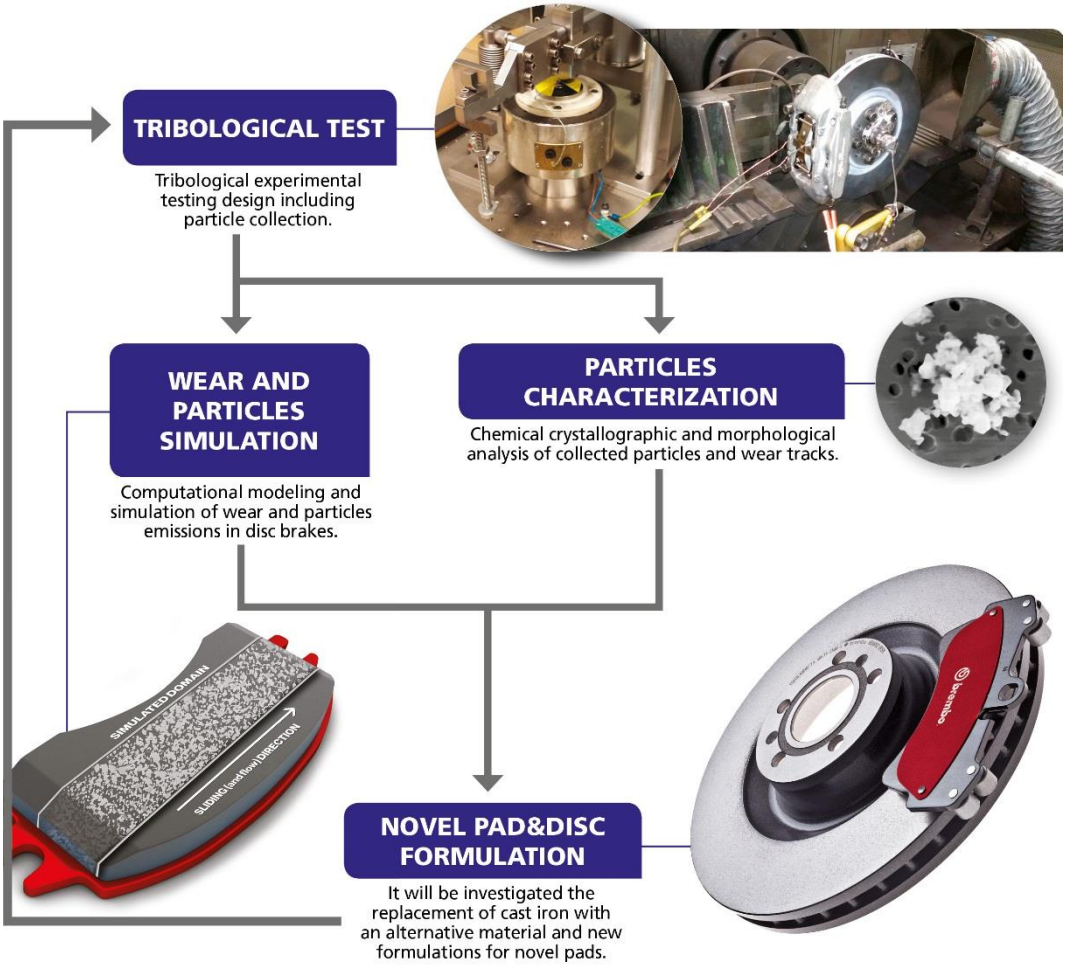

Fig. 1 Overview of the REBRAKE project.

The development and validation of the new concepts concerning friction and disc materials were conducted using an inertia disc brake dynamometer test set-up in parallel with pin-on-disc (POD) instruments: these tests were used to evaluate the influence of the friction material and disc surface properties on PM_{10} emissions at the system level and at the material level respectively. At the material level, two POD set-ups were used: in the first POD set-up (**Fig. 2,** [25]), the contact temperature was increased by ramping up the applied load from 1 to 7 kg, corresponding to applied pressures from 0.1 to 0.9 MPa, considering that pins with a 10 mm diameter were used. A second POD with an external heating coil that raised and stabilized the disc temperature to the set values was also used in the project. At the system level, a specially designed and dedicated dynamometer [26], [27] test set-up was developed for measuring emissions (**Fig. 3**). An ELPI+®cascade impactor was used to both collect and count in real-time particles in 14 size stages (from 6 nm to 10 µm) at a sampling frequency of 1 Hz [28]. Controlled clean air was supplied using HEPA filtered air flushing in the dynamometer box built around the brake assembly at a flow rate of 1175 m^3/h, while in the case of the POD, the air flow was 2.2 l/s, providing an air exchange rate of 1.3/min. Moreover, in the case of the dynamometer, isokinetic sampling with high sampling efficiency was implemented.

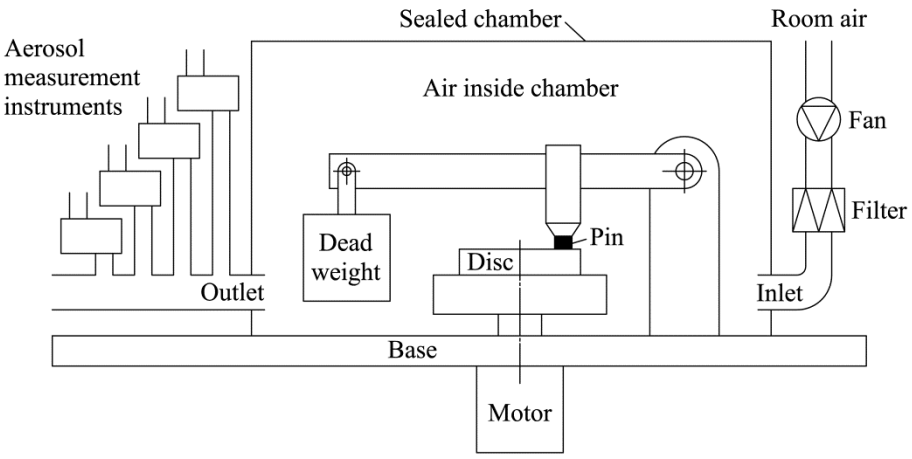

Fig. 2 Schematic on PoD set-up for particle collection and relevant aerosol measurement during wear tests.

Fig. 3 The instrumented dynamometric test rig with all the equipment needed for PM sampling and collection. (R) rotor; (C) dust-box chamber; (T) outlet tube; (F) inlet tube from which clean air enters; (BB) bigger box (door open).

The data provided by POD tests were used as input for Finite Element Analyses (FEA) and Cellular Automaton (CA) simulations: these tools worked on different length scales, from macroscopic down to mesoscopic.
In parallel, a multi-analytical characterization approach based on: optical microscopy, scanning and transmission electron microscopy (SEM and TEM, respectively), energy dispersive X-ray spectroscopy (EDXS), and focused ion beam (FIB) equipment was developed and used [29] for the characterization of wear products. The structural characterization of the wear products was conducted by X-ray diffraction (XRD) which with data processing based on the Rietveld method provided microstructural parameters and phase composition [30]. The outer surface of the friction layers was investigated with Raman spectroscopy [31].

MATERIALS

A front left disc brake assembly schematic, representative of a typical medium-size European passenger car [32] is depicted in **Fig. 4** and includes: i) a ventilated disc brake (R) made of cast iron [33]; ii) an aluminium fixed calliper (FC) with four pistons; iii) two brake pads (P) [34], [35], [36].

The disc was made of grey cast iron with a 4.1% carbon equivalent content and a hardness of 210 ±10 HB. The matrix was fine lamellar pearlitic with a distribution of at least 70 % type A (graphite flake structure). This same material was used for POD, dynamometric and car tests. Following preliminary PoD investigations [37], [38], a standard hardening treatment procedure was adopted for the disc, characterized by heating it up to 860 °C for 2 h under a controlled atmosphere. Subsequent oil quenching and tempering for 4h at 180°C increased the cast iron hardness from the initial 210 ±10 HB (untreated condition) to 473 ±25 HB (heat-treated condition).

Friction materials are classified according to their metal content and the resulting range of the coefficient of friction (CoF). The total Fe and Cu content of Non-Asbestos Organic (NAO) friction materials is typically lower than 10% and the CoF is quite low. Very Low-Steel materials (with total Fe and Cu content typically in the range 10-50%) are derived from NAO materials and have an improved braking efficiency. NAO and Very Low-Steel materials are commonly used in the US and Japan markets [35]. Low-Steel materials contain not only higher concentrations of Fe and Cu, but also higher concentrations of abrasives. For this reason, the higher resulting values of the friction coefficient are often accompanied by relatively higher brake wear and noise [39]; low-steel friction materials are produced for the European market instead. Five friction materials code-named M1, M2, M3, M4 and M6 representing the main classes of commercial products nowadays available on the market were investigated. Phase composition of studied friction materials was determined using the XRD technique and identified phases are listed in **Table 1**. Pad M3 is very common in the European market: for this reason, M3 was taken as the reference benchmark for the project. It is worth noticing that this material features quite a large copper concentration. The other Low-Metal materials were selected primarily to cover a comparatively wide range of brake performances, as inferred from the content of their abrasive components.

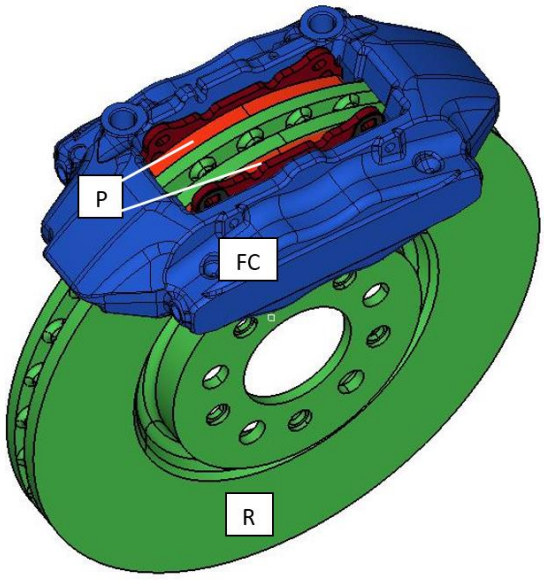

Fig. 4 Schematic of the disc brake assembly: (R) cast iron rotor; (FC) aluminium fixed calliper; (P) low steel brake pads.

Table 1: Phase compositions, as evaluated from XRD data, of the friction materials investigated within the REBRAKE project. The percentage of the organic phenolic binder is not accounted for. Silicates refer to "clay minerals" whose actual structure and composition are different in different friction materials.

Phase (%Wt)	M1	M2	M3 (reference)	M4	M6
Zinc – Zn	14.31	9.68	5.61	18.19	5.08
Graphite – C	39.28	26.51	33.00	35.69	31.98
Copper – Cu	11.16	16.03	35.93	11.45	9.00
Silicates– $(K,Na)(Mg;Fe)(AlSi_3O_{10})(OH)_2$	6.93	1.17	1.50	1.65	9.42
Potassium Hexatitanate– $K_2Ti_6O_{13}$	0.75	11.07	0.00	2.04	8.37
Barite - $BaSO_4$	0.00	7.85	8.08	0.00	22.88
Baddeleyite - ZrO_2	0.00	23.16	0.64	2.50	9.85
Fe-alfa – Fe	3.52	3.67	4.60	7.56	0.93
Moissanite - SiC	1.80	0.00	0.00	0.00	0.00
Chromite - $(Fe, Mg)Cr_2O_4$	5.61	0.00	1.45	2.51	0.00
Zincite – ZnO	2.25	0.15	0.00	0.00	0.00
Berndtite - SnS_2	2.46	0.00	0.77	1.80	1.13
Periclase – MgO	5.89	0.00	3.17	12.76	0.00
Sphalerite - (Zn,Fe)S	1.71	0.45	0.00	1.31	0.00
Corundum - Al_2O_3	4.33	0.26	2.76	2.53	1.36
Stibnite - Sb_2S_3	0.00	0.00	2.50	0.00	0.00

The diversity of studied friction materials is well demonstrated in **Table 1**. It is clear that M1 consists of the highest amount of hard abrasives (Al_2O_3 and SiC) accompanied by mild abrasives (MgO and $(Fe,Mg)Cr_2O_4$). The M1 formulation is considered to have the most abrasive character while the abrasive effect of this friction material is balanced mainly by the presence of graphite and metal lubricants SnS_2 and (Zn,Fe)S. The M3 (reference) friction material contains a significantly lower amount of abrasives Al_2O_3, MgO and $(Fe,Mg)Cr_2O_4$ than M1 and the abrasive character is modified by the presence of graphite and Sb_2S_3 as typical solid lubricants and, together with a high amount of Cu, predetermines this material for smooth friction behaviour. Al_2O_3, MgO, ZrO_2 and $(Fe,Mg)Cr_2O_4$ are present as abrasives in the M4 formulation and graphite, SnS_2 and (Fe,Zn)S present typical solid lubricants in this formulation. Based on the composition, the friction materials M1, M3 and M4 are classified as low-steel friction composites. The formulation of the M6 friction material is very different from M1, M3 and M4 with high amounts of ZrO_2 accompanied by low amounts of Al_2O_3 as hard abrasive. The friction behaviour is balanced by the graphite, $BaSO_4$ and $K_2Ti_6O_{13}$. The M6 formulation is the typical one for non-asbestos organic (NAO) friction materials. M2 friction material consists of obviously high amounts of ZrO_2 and low amounts of Al_2O_3 and the abrasive character of this formulation is balanced mainly by the presence of graphite, $K_2Ti_6O_{13}$ and also $BaSO_4$. This material is therefore close to the M6 friction composite whereas M2 consists of significantly higher amounts of metallic iron typical of low-steel formulation (M1, M3 and M4).

RESULTS - POD TESTS

All friction materials used in the present investigation contain a phenolic resin as a binder. Therefore, a transition in wear behaviour when the contact temperature is increased is expected, due to the progressive degradation of the phenolic binder [40], [41], [42], [43]. This aspect is paramount since it concerns the evolution of the wear regimes and relevant emission of airborne particles. **Fig. 5** shows comparatively the tribological behaviour of materials M1, M2 and M6 as the test temperature was externally increased from room temperature to 300 °C. The expected

transition from mild to severe wear occurred at disc temperatures between 180°C and 250°C, depending on the material. As an example, in **Fig. 6a)**, the cross sectional view of the worn out pin of the M2 material is shown. The top friction layer is the result of the compaction of the wear debris trapped in between the mating surfaces of the pin itself and the rotating disc in agreement with literature studies [31], [38]. The planar view of the same specimen is shown **Fig. 6b)**. The picture emerging displays a friction layer with heterogeneous microstructure, featuring more or less compacted debris, depending on the local and instantaneous mechanical coupling conditions.

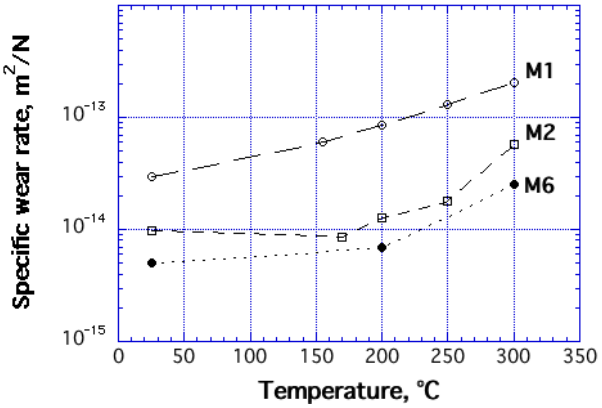

Fig. 5 Specific wear rate for M1, M2 and M6 materials from pin-on-disc tests as a function of the disc temperature (external heating).

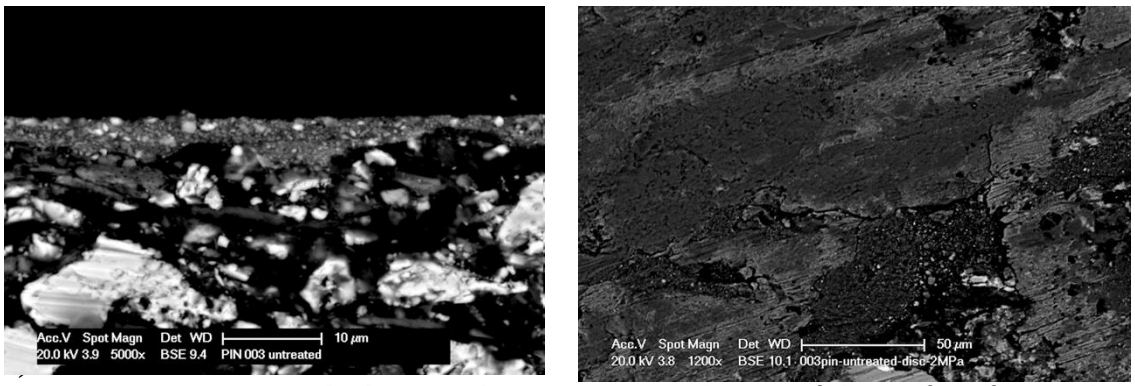

Fig. 6a) SEM micrograph showing the cross sectional view of the surface friction layer that forms on the pin made of M2 friction material. b) Planar view of the same specimens. The heterogeneous structure of the friction layer can be better appreciated.

From this comparative investigation, the important role of the abrasive components, such as MgO, in determining the wear behaviour of the relevant friction material, emerges. With regard to MgO, it is absent in the M2 material which exhibits a lower wear rate than M1 in which MgO is present. In addition to that, the lower wear rate displayed by M2 compared with M1 is also due to a better performing friction layer building up on the M2 pin surface. According to literature data [44], specific components in the right concentrations are required for the formation of a stable friction layer. One of the most effective formers of friction layers is ZrO_2, which is present in M2 and M6 but not in M1 (see **Table 1**). The best performances of M6 seem to rely heavily on the particularly high concentration of barite in combination with a high content of potassium hexatitanate. Barite, generally classified as a filler [35] could be an important component of a stable friction layer, on the other hand, the positive effect of potassium hexatitanete on the wear rate has already been described [45]. In actual fact, for the formation of a friction layer that preserves a sufficient stability also at high working temperatures, the presence of copper, in the form of fibres and powders, is crucial [46]. This

element is present in all REBRAKE friction materials (**Table 1**) and it was a focal point of the project [47].

Using the POD with frictional heating, the experiments show that as the temperature increases from 100 °C to 300°C, the emission of ultrafine particles intensifies while that of coarser particles decreases. **Fig. 7** shows the plots of the particle concentration (C) and total PM_{10} vs time for tests performed on the M4 friction material at a disc temperature of 129 °C and 245 °C. The behaviour of PM_{10} emissions changes by a factor of 3, although the trend of C is drastically different. C is given in hundreds/cm^3 at 129 °C and in millions/cm^3 for the test performed at 245°C. There is a critical temperature, T_u, at which the rate of ultrafine particle emission rises stepwise by 4 to 6 orders of magnitude. This transition is reversible and the concentration decreases when the temperature decreases.

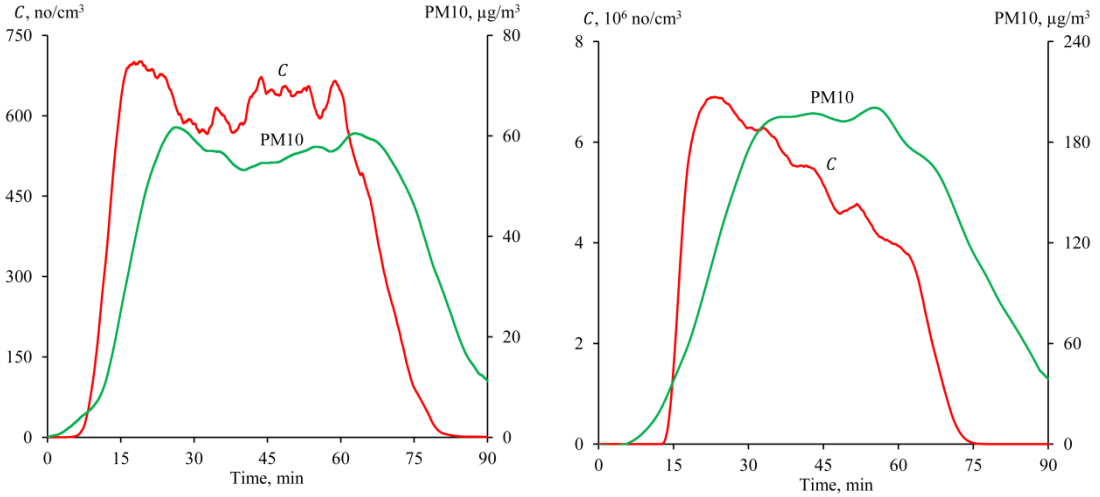

Fig. 7 Left; Particle concentration and PM_{10} at temperatures below T_u (M4, 1 MPa × 1.6 m/s, T_s = 245 °C). Right; Particle concentration and PM_{10} at temperatures above T_u (M4, 0.5 MPa × 1.6 m/s, T_s = 129 °C).

Fig. 8, referring to M2, shows how T_u can be graphically evaluated. This critical temperature ranges from between 165 °C and 190 °C. Below this temperature range, fine particles outnumber coarse and ultrafine particles, although coarse particles make up the bulk of the particulate matter mass. Above the critical temperature, ultrafine particles constitute almost 100% of the total particle number and their relative mass contribution can exceed 50%. The critical temperature values were found to be correlated to the transition temperatures from mild to severe wear (**Fig. 5**).

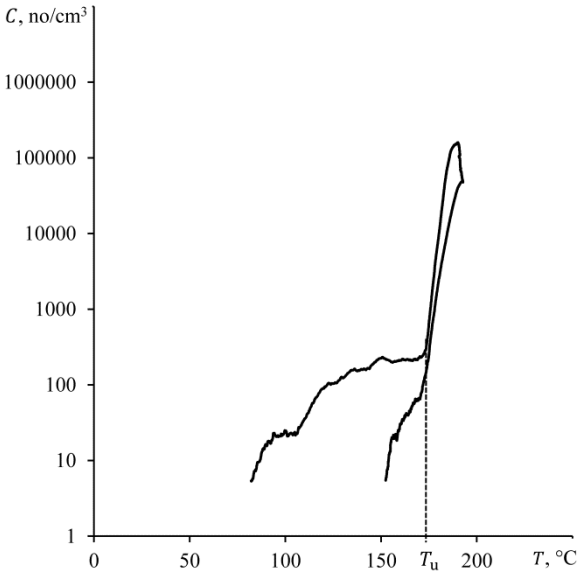

Fig. 8 Particle concentration vs temperature for M2 friction material. The critical temperature is marked as T_u .

The effective density of airborne wear particles from car brake materials was investigated, using the POD equipment schematized in **Fig. 2**. Two methods were used to determine the effective density. The first method is based on measurements of the total PM_{10} emissions and particle size distribution. The second involves measurements and subsequent fitting of the mobility and aerodynamic size distribution. For this purpose, one of the outlet air ducts (see **Fig. 2**) was connected to instruments that measure the mobility and aerodynamic size distributions as well as the PM_{10} emissions [48]. The results obtained with the two approaches show good agreement, and an effective density of $0.75 \pm 0.20 g/cm^3$ was estimated. Note that this is a typical value for atmospheric aerosols collected near traffic arteries [49]. The effective density decreases with a POD test temperature that increases from 110 °C to 360 °C. There is a comparatively large difference between the effective density and the theoretical density of the particle material. Both particle porosity and shape affect the effective particle density [50] which suggests that the particles are porous or have an elongated shape. To investigate these aspects, particles emitted from the M1-vs-cast iron friction pair were collected on ELPI+Al foils [51]. SEM observations show that most of the 0.1−0.9 μm particles, with a width-to-length aspect ratio of 0.7 ± 0.2, are actually clusters of smaller ones, involving interstitial voids whose presence is fully compatible with their lower density, compared with a full dense material. Particle porosity was determined by FIB-sectioning

single particles in order to expose and analyse their cross-section.

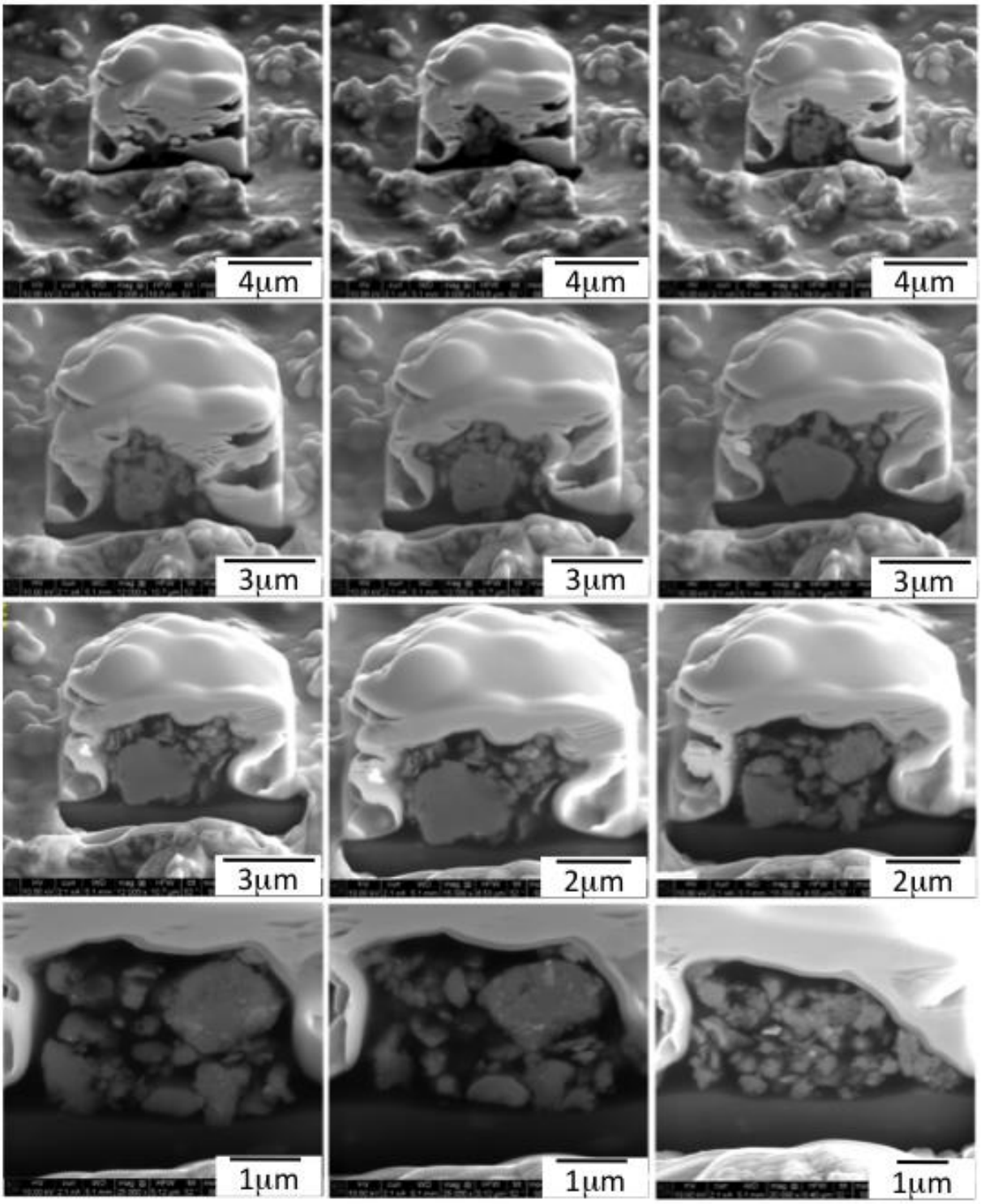

Fig. *9* shows the sequence of images obtained with a single particle ion-sliced with a step of approximately 300 nm. The sample preparation procedure consisted in the deposition of a gold coating and a platinum patch over the substrate containing the particles. The porosity of a particle was determined by analysing a number of its cross-section images. The domains of 'voids' and 'solid material' were obtained by image analysis. Most of the 0.3−6.2 μm particles revealed an effective porosity of 9 ± 6 %. On the basis of the results obtained from the analysis setting relationships between the effective particle density, particle material density, dynamic shape factor and porosity, it was concluded that the shape factor has a stronger influence than porosity itself on the effective density of airborne wear particles. The dynamic shape factor is defined as the ratio of the drag force on a non-spherical particle to the drag force on its volume

equivalent sphere, assuming that both move at the same velocity with respect to the atmosphere [52]. These results are definitely interesting for an accurate prediction of the behaviour of the particles suspended in the atmosphere and their path inside the pulmonary system of humans.
In the two mentioned studies [48], [51], airborne particles from brake materials with diameters exceeding 6 nm were investigated. To obtain information also on smaller particles, with an average aerodynamic diameter in the 1–10 nm range, particularly as concerns their number fraction, an additional study was performed [53].
The airborne nano-particles were captured and analysed using a nano-Condensation Nucleus Counter (nCNC), which allows the counting of particles with diameters from 1.3 nm to 1 μm. nCNC was used in parallel with a Condensation Particle Counter (CPC). The CPC counts particles that are larger than 10 nm. In this way, three intervals could be classified: particles larger than 1.3 nm, particles larger than 4.4 nm, and finally particles larger than 10 nm.
With reference to **Fig. 10**, which refers to M6 friction material, it turns out that at temperatures above 160 °C, the nanometric particle emission rate increases abruptly. Very similar results were also observed with the other friction materials, thus confirming a general trend dominated by the decomposition of the phenolic binder. Moreover, 160°C is a temperature that is consistent with the transition temperature observed in the wear rate vs T curves obtained in the POD tests using external heating of the disc (**Fig. 5**). This result shows the strict relationship between wear rate and PM emission, as demonstrated in the following with reference to dynamometric tests.

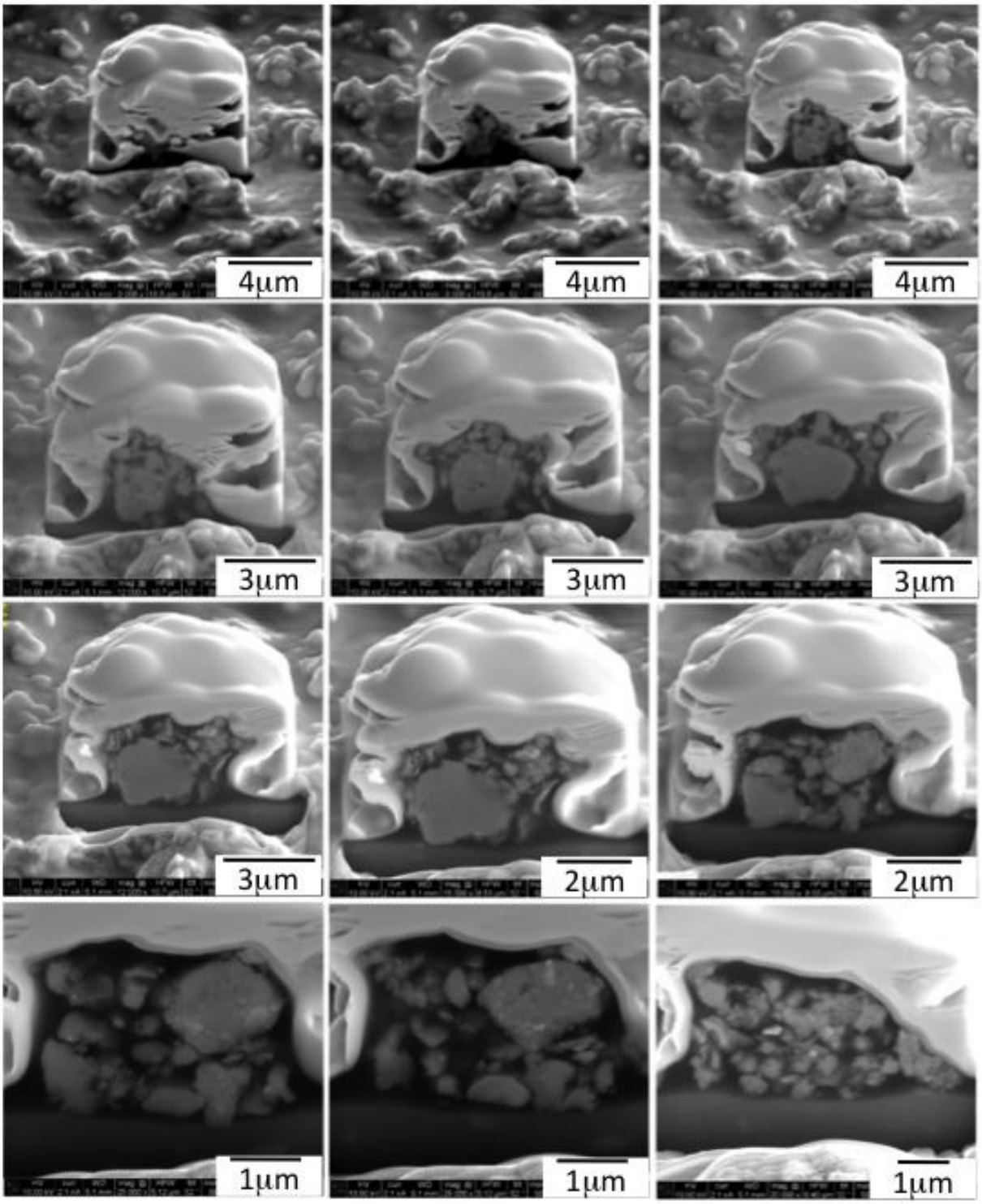

Fig. 9 SEM images of the agglomerated particle cross-section under analysis after FIB etching intervals of approximately 300 nm (unpublished figure, acknowledgment to Rafael Borrajo-Pelaez KTH – Materials Science). Friction material M1 collected on an ELPI+ stage without grease.

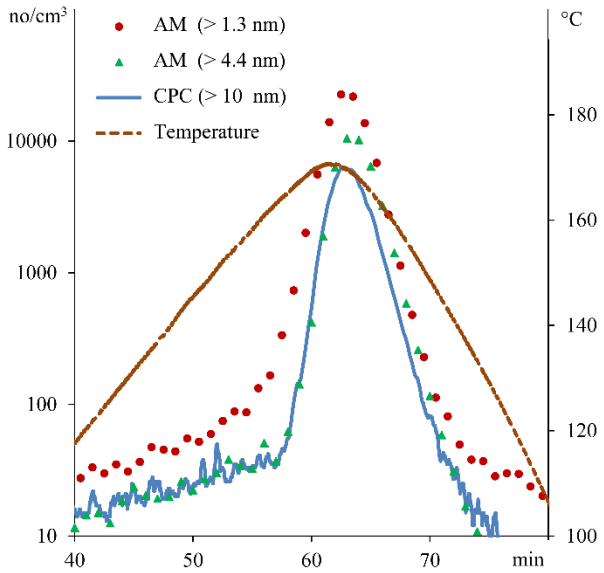

Fig. 10 Nanometric particle concentrations for M6 pin wear tested against cast iron discs. AM (> 1.3 nm) number of particles larger than 1.3 nm. AM (>4.4 nm) number of particles larger than 4.4 nm. CPC (>10 nm) number of particles larger than 10 nm.

At temperatures that are lower than 160°C, an important contribution to the wearing out of the sliding system comes from the disruption of the friction layer and abrasion exerted by the harder oxide particles, trapped between the mating surfaces. These abrasive components are also able to furrow the cast iron disc, leaving behind typical surface scratches.
Although the average recorded contact temperature is comparatively low, limited oxidation can still take place and hematite (Fe_2O_3) mainly and magnetite (Fe_3O_4), are detected in the wear debris iron oxides. Any temperature rise above the transition temperature induces important structural changes in the phenolic binder. The larger amount of the wear debris coming from the pin and tribo-oxidation of the disc contributes to the formation of a more stable, widespread friction layer. Wear debris does not "immediately" abandon the system, as mainly happens at the lower loads, featuring loose debris (**Fig. 11a)**, 1 kg)). At higher loads, they are trapped and compacted in between the pin and the disc mating surfaces to form secondary plateaus in the friction layer. Fragments of these plateaus are subsequently emitted and are collected by the ELPI+ impactor (**Fig. 11b)**, 5 kg)).

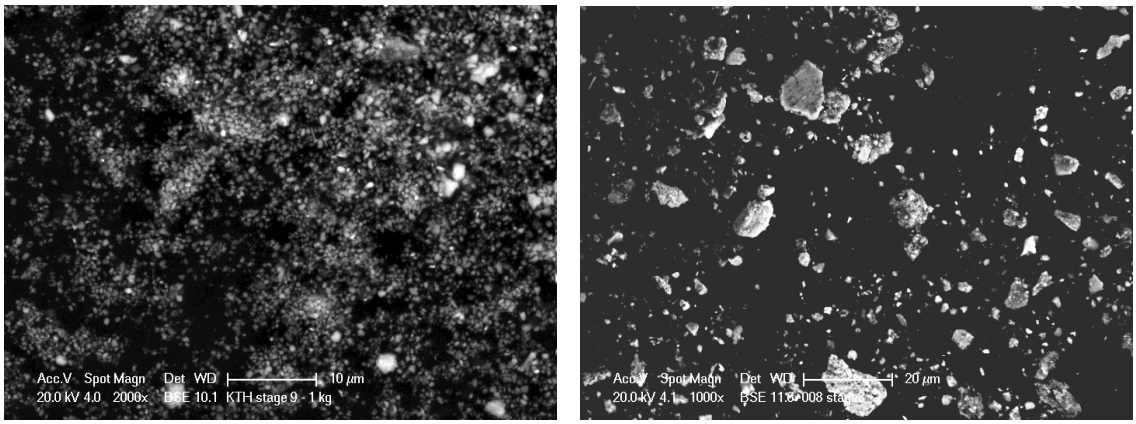

a) b)

Fig. 11 Wear debris collected on stage 9 of the ELPI+ impactor during the POD tests conducted with M1 friction material, sliding against a cast iron disc, below, a), and above, b), the transition temperature, corresponding to a 1 kg and 5kg applied load respectively.

At the end of the POD tests, the ubiquitous presence of a carbonaceous layer was also detected on the surface of the friction material specimens using Raman spectroscopy [31]. The structure and micromorphology of this surface layer is the result of the complex interactions occurring under the joint effect of thermal activation and shear mechanical stress between the organic binder, graphite, particles and fibres, and carbon coke additions to the phenolic resin. These aspects, as described below, were investigated further, scaling up the experimentation to dynamometer tests level.
The results obtained from the characterization of the wear products were used to achieve a broader understanding of the dominant tribological mechanisms and how they are affected by the actual interface parameters such as roughness, real contact area, frictional and external heating contact temperature [54].

RESULTS - DYNAMOMETRIC TESTS

The dynamometric tests were run following a cycle based on the modified SAE J2707 Method B. The modifications mainly consisted of avoiding *highway* and *hill-descending* blocks since they are not relevant to urban conditions. Moreover, a reduced number of brake stops for each block was used: the total number of stops was 200 [55].
The particles collected display remarkably common features to those coming from the POD test rig. As an example, in **Fig. 12**, the TEM micrograph (a) and relevant X-ray map (b) of an M1 cluster of debris collected on ELPI+ stage 5 (corresponding to collected particles with average size below 108 nm). As a general comment, it is interesting to note that also in the ultrafine size range, the emitted particulate tends to cluster together to form larger composite grains.

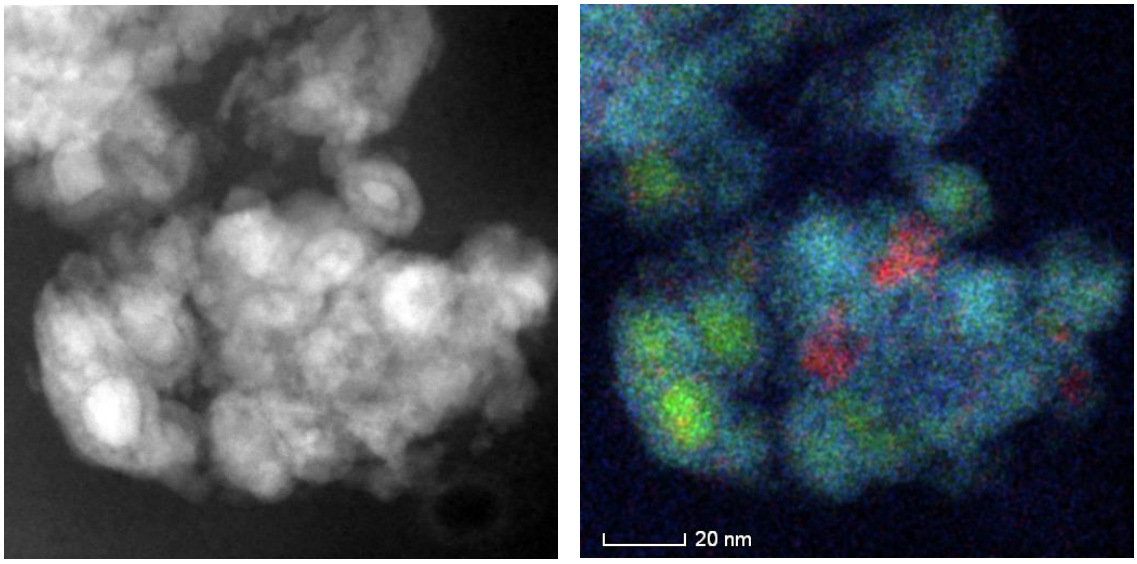

Fig. 12 Wear debris collected on the stage 5 of the ELPI+ impactor during the dynamometric tests conducted with M1 friction material, sliding against a cast iron disc a) TEM micrograph; b) EDXS map of the main detected elements. Colour code: green – Fe; red – Cu; blue – O (oxide). The main features are the core-shell structures, displaying an inner part containing metallic iron, surrounded by a native iron oxide layer. These particles are clustered and held together by a mixture of oxides and copper intergranular inclusions.

In

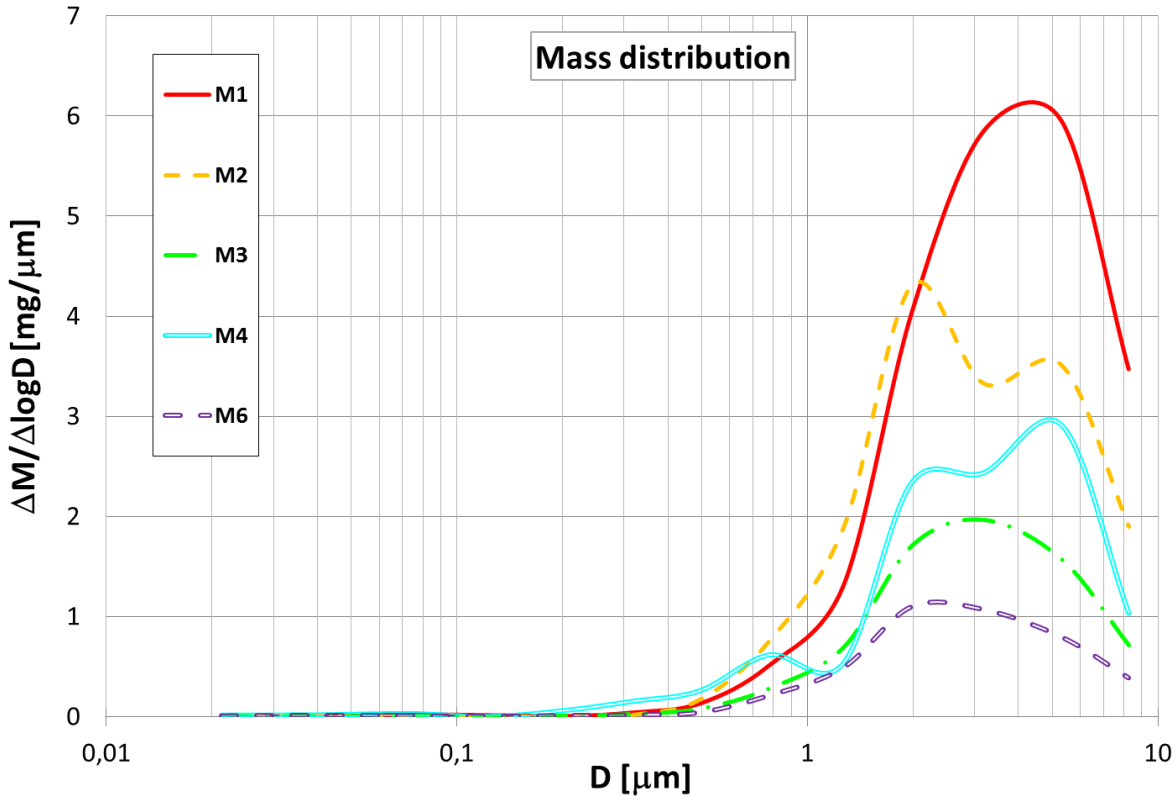

Fig. 13 the emission curves for the friction materials presented in T**able 1** are displayed. These results show that there are notable differences in PM (size range 1-10 µm) emission for the different friction materials. In particular, it turns out that compared with M3 (the benchmark friction material), M1, M2 and M4 exhibit larger PM emission curves over the whole range of airborne particle size. A significant reduction is achieved, on the other hand, by M6, whose emission curve lies below the M3 curve, indicating a reduction in the total amount of emitted airborne particulate as was expected since M6 is an NAO material [14]. Since all the 15 stages of the ELPI+ impactor are used for the PM_{10} collection, the total amount of PM_{10} generated can be expressed as [27]:

$$PM10 = \frac{1}{f}\sum_{i=1}^{15} PM_i \qquad \text{Eq. (1)}$$

where f is the volume fraction of aerosol sampled (f=1/1958).

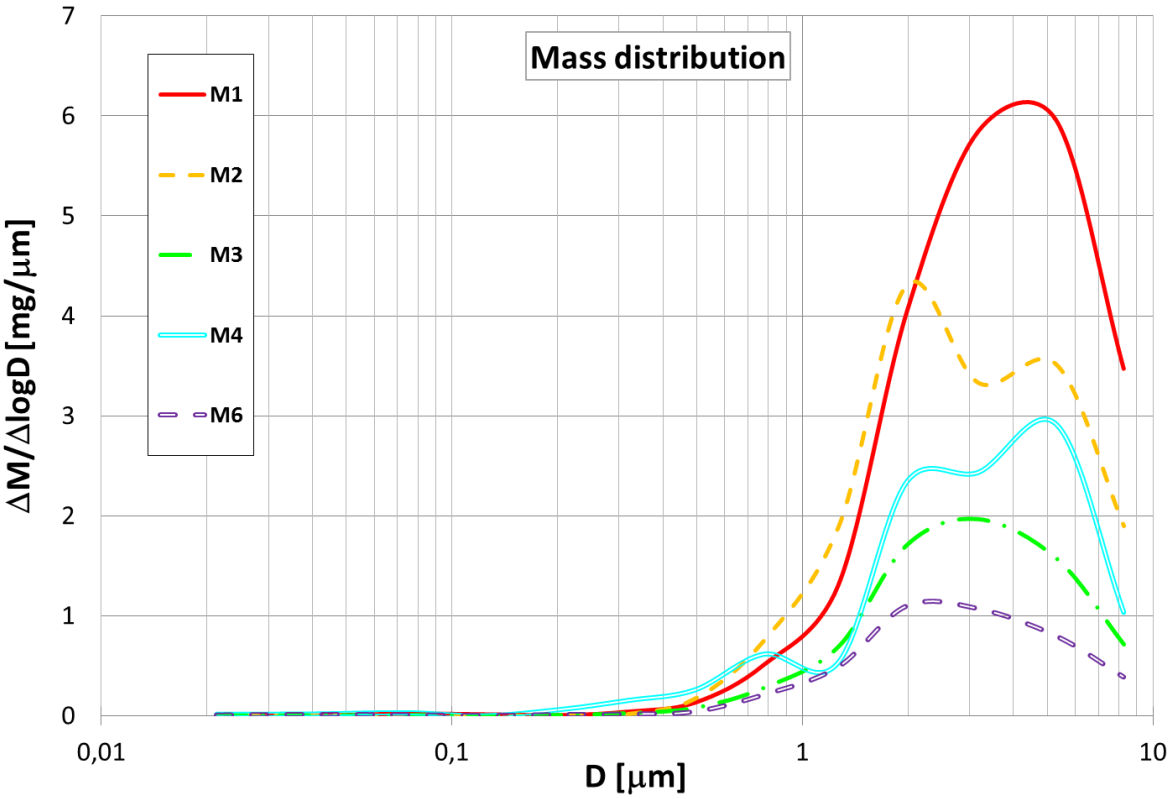

Fig. 13 Mass distribution vs size of PM collected by the ELPI+ foils during the dynamometric tests with the five friction materials (Table 1).

In **Table 2**, the PM emission parameters obtained by dynamometric testing of the five studied friction materials are listed together with the relevant tribological parameters –the PM_{10} emission factor, expressed as the amount of airborne particulate matter emitted for each stop from one front disc brake system is also reported [27]. The data for the friction materials tested against cast iron discs have also suggested an effective development strategy for this research: in fact, considering the same order of contribution to the total PM_{10} emission of the pads and the disc, the need to also improve the tribological and emission performances of the discs is evident. Following up preliminary investigations based on POD tests [37] that defined and assessed effective heat treatment parameters and resulting disc conditions, real size cast iron discs were therefore subjected to the same thermal treatment as POD samples. The surface hardness and the microstructural features obtained in real discs were the same as those found in POD parts. For this reason, in addition, **Table 2** presents the results for the best performing friction materials, M3 and M6, when they are tested against heat-treated discs.

Table 2: Summary of the results obtained from dynamometric tests on the five friction materials M1-M4 and M6, tested against cast iron disc, and M3 and M6 tested against *heat-treated* discs.

	M1	**M2**	**M3 (benchmark)**	**M4**	**M6**	**M3 – *Heat-treated***	**M6 –*Heat-treated***
Tribological parameters							
Average CoF	0.42	0.38	0.37	0.39	0.34	0.39	0.34
Disc mass loss, g	8.3	3.8	3	5.8	0.4	2.8	0.4
Pad mass loss, g	6.6	11.6	4	6.94	4.54	3.9	3.3
Total mass loss,	14.9	15.4	7	12.8	4.9	6.7	3.7

Emission parameters							
Total PM_{10}, g	9.27	7.2	3.3	6.7	1.8	2.26	1.17
PM_{10}emission factormgstop^{-1} brake^{-1}	46	36	16.5	33.5	9	11.3	5.8

The results presented in **Table 2** show that by improving the quality of the cast iron rotor using a thermal-treated disc that is comparatively cheap and, most importantly, potentially compatible with industrial production, the total PM_{10} emission can be reduced by 32% using the same friction material (M3); it is also evident that when using a combination of NAO friction material, such as M6, and the same heat-treated disc, the total PM_{10} emission during dynamometric tests designed according to a typical urban cycles is further reduced by 65% compared with the benchmark material (M3) under identical testing conditions.
To complete the picture of the results obtained from dynamometric tests, the existence of a transition temperature also on full scale disc brake systems is confirmed [56]. Above this temperature, a major increase in PM emission was recorded. This behaviour is certainly influenced by the decomposition phenomena occurring in the phenolic resin, as demonstrated by the POD studies [31], [57], [58], [59].

RESULTS - NUMERICAL MODELLING and SIMULATION

A major challenge when numerically simulating the disc brake contact is that different phenomena occur at different size scales, making it critical to choose models that adequately describe the studied contact situation. Disc brake wear was numerically simulated using various approaches. Finite element analysis (FEA) is the usual approach for simulating macroscopic disc brake contact [60], [61]. The advantage of FEA is that several commercial tools can handle thermal–mechanical models and are also used in industry. However, it would be difficult to simulate the plateau dynamics, as occurring on the pad-disc interface, using FEA only since typical length and time scales are in the order of millimetres. Müller and Ostermeyer [62] have developed a cellular automaton (CA) approach for describing the plateau dynamics on a mesoscopic scale and Österle and Dmitriev [63] have developed a movable cellular automaton (MCA) approach for numerically simulating the frictional behaviour of the friction layer at the micrometric scale. Due to the short length and time scales needed in the mentioned CA and MCA approaches, scaling up to macroscopic behaviour is rather difficult. Numerically simulating how the mesoscopic contact situation affects macroscopic disc brake behaviour requires a numerical approach that can handle braking events in seconds and disc and pad lengths in centimetres. With this in mind, Wahlström et al. [64] started to develop a CA approach that can be used to determine the amount of wear material leaving the disc brake contact. This approach could be used to simulate braking time in the order of seconds and lengths in order of centimetres and it correlates qualitatively with the experimental observations presented by Eriksson et al. [65].

Within the REBRAKE project, both FEA and CA models were developed to investigate the possibilities of using both methods to study the contact conditions and wear propagation in disc brakes.

FEA Simulation Approach

The wear simulation approach proposed by Söderberg et al. [60], [61] was implemented in the FEA of both the POD [66] as well the dynamometric bench set-up [67]. Friction and wear

models based on the experimental results obtained within REBRAKE [57], [58], [59], [68] were implemented in the models.
The finite element discretization of the POD considered wear of the pin specimen and included thermal effects. Comparison between simulated and experimentally observed wear propagation showed good agreement after steady state conditions were reached, but the FE simulation was not able to capture the initial running-in process.
In the simulation of the dynamometric bench set-up, the calliper, brake pads and rotor were included in the FE-model (see **Fig. 14**). Contact pressure distribution and wear propagation were predicted for the REBRAKE dynamometric bench test cycle. Wear on both pads and rotor was considered in the simulation (see **Table 3**). Good agreement between test and simulation, as concerns the average value of wear rate for both disc and pad, was achieved, considering that the disc and pad wear have uncertainties equal to one unit on the latest significant figure of each relevant value in **Table 3**.

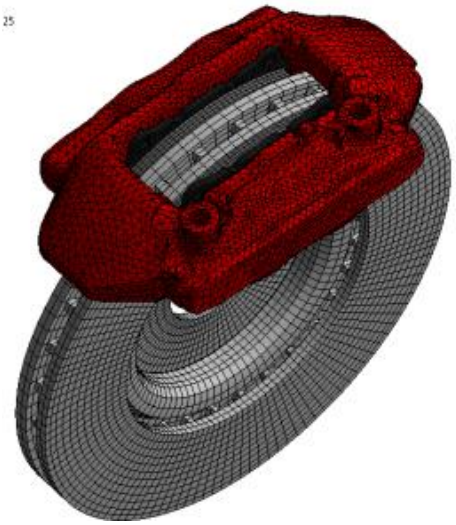

Fig. 14 FE mesh of disc brake system used to simulate pressure distribution and wear of the pad and rotor contact.

Table 3: Average wear loss of disc and pad of FEA simulated and experimentally run test cycle

	Disc mass loss [g]		Pad average wear [mm]	
	Simulation	Measured	Simulation	Measured
M1	8.3	8.3	0.24	0.22
M4	5.8	5.8	0.18	0.21
M6	0.4	0.4	0.08	0.10

CA Simulation Approach
The aim was to develop the CA approach further by implementing friction, wear, and particle emission models based on data found in the literature and integrated with our experimental results [69]. The wear and temperature of the disc surface is also important since it will change the gap between the pad and disc surfaces which affects how the wear particles will flow and in turn, the plateau formation dynamics. For this reason, the model was also extended to the disc, being part of the contact [70].
By comparing dynamometric bench results with the same measures, the validity of the CA simulations could be investigated. The CoF measured during a dynamometric test and the simulated mean CoF are of the same order and display a similar trend, which is also the case for the measured and simulated bulk temperatures of the pads and disc. Similar agreement was found between the measured airborne volume losses of the pads and disc and the relevant

simulated value. The shapes and dimensions of the contact plateaus were of the same size order as the simulated ones.
These comparisons together indicate that the CA approach is able to explain what occurs at the pad–disc contact on a mesoscopic scale during braking and that the simulated surface profiles, contact pressure, and contact temperatures might also be predictively used to study how different metal fibre orientations and morphologies affect the local transient contact state and predict how they will affect the behaviour of the disc brake in terms of friction and wear. However, we are well aware that the simulation approach needs to be developed further to be able to obtain a quantitative correlation with the experimental results.

GENERAL DISCUSSION AND FUTURE PERSPECTIVES

One of the main goals of the REBRAKE project was the demonstration of the possibility of reducing PM_{10} emissions from automotive disc brakes by at least 50 wt.%. To get an idea of the importance of this issue, just consider that if emissions from disc brake systems were reduced by 50 wt.% on vehicles circulating in Europe, this would reduce the overall PM_{10} emissions from road traffic by 4-14 %. In the REBRAKE project, the results demonstrate that it is possible to design a brake system that can reduce PM_{10} emissions by up to 65 wt. %. This result has been achieved (**Table 2**) with a solution including NAO brake pads and a thermally treated disc by optimizing the composition of the pad friction material and tuning the mechanical properties of the cast iron discs. Whether this disc treatment is compatible with an industrial large-scale production and whether all customers are ready to accept NAO friction materials, especially in the markets were they are not currently used, as in Europe, still has to be assessed . It has to be said that, in addition to the performed tests which focused on the evaluation of PM_{10} emissions, there is a need to run subsequent series of dynamometric tests (performance, crack resistance, noise behaviour and many others) as well as test at the vehicle level to allow this friction pair in real cars.

The selection of the right components for developing new friction materials relies on a precise understanding of the fundamental aspects of the tribological behaviour of the disc-pad systems. Full comprehension of the wear mechanisms active in brake systems and their effect on the relevant emission behaviour achieved within REBRAKE has lead to a better understanding of the direct correlation with the composition of the brake components, pads and discs: this is a prerequisite to developing new low emission braking materials. This has to be achieved in conjunction with the elimination of environmental critical components from commercial friction material and replacing them with “green” products. Indeed, the knowledge acquired within REBRAKE on the working principles and critical features of the disc-pad supports the methodologies for the replacement of components, such as copper and others, which are potentially dangerous for the environment and human health [19], [20], [71].

The combined simulation and testing methodology that has been developed and continuously tuned during the project is extremely important for an enhanced understanding of the mechanisms of formation of the airborne particulates from disc brakes, as well as the development of new concepts that can reduce the PM_{10} airborne mass.

Another important methodological output of REBRAKE is a first attempt to determine the density of aerosols generated by disc brake systems. This is a main issue given that a strong contribution to the total weight of the airborne emissions by the wear debris comes from the brake disc. The high concentrations of iron oxides are mostly produced by the abrasion and tribo-oxidation of the cast-iron discs. This justifies the fact that an improvement in the wear resistance of the discs would beneficially influence wear resistance and particle emission:

further research is ongoing to improve materials, surface treatments and coating systems of the discs in order to limit their contributions to particulate matter emission.

A more effective approach to further reduce emissions from car brake systems should rely on a holistic approach in which the search for innovative materials, i.e., friction materials, disc treatments and disc coatings, is certainly an important prerequisite to reduce emissions without jeopardizing the effective braking action. However, in the future, this is not the only element to be considered. For example, an important fraction of these emissions might be captured soon after their formation, with appropriate on-board devices mounted close to the pad-disc interface. Also developing braking "best practices" is another fundamental aspect to exploit the potentialities of materials used in advanced braking systems to the full. For example, through a smart dashboard, drivers may adjust their individual braking style in order to reduce brake emission and at the same time prolong the overall lifetime of the brake materials. This human-based element could be expanded further by the optimization of car sensors.

All these combined approaches will be included in the REBRAKE's companion Project: LOWBRASYS (a LOW environmental impact BRAke SYStem, [72]) which by September 2018 will provide the design and prototype of an innovative brake system.

Acknowledgements
The research leading to these results has received funding from the European Union Seventh Framework Programme (FP-PEOPLE-2012-IAPP) REBRAKE Project, under grant agreement no. 324385 (www.rebrake-project.eu). At the end of this 4-year project, several colleagues and friends deserve to be acknowledged for their support – our warmest appreciation goes to all of them.

REFERENCES

[1] M. Gasser, M. Riediker, L. Mueller, A. Perrenoud, F. Blank, P. Gehr, B. Rothen-Rutishauer, Toxic Effects of Brake Wear Particles on Epithelial Lung Cells in Vitro," Partic. Fibre Toxicol. 6(30) (2009).
[2] Exceedance of air quality limit values in urban areas (Indicator CSI 004), European Environment Agency, 2016.
[3] T. Grigoratos, G. Martini, Brake Wear Particle Emissions: a Review, Environ Sci. Pollut. Res. 22, (2015) 2491−2504.
[4] Traffic and air quality contribution of traffic to urban air quality in European cities, Hak, C., Larssen, S., Randall, S., Guerreiro, C., Denby, B. and Horálek, J., Technical Paper 2009/12, European Topic Centre on Air and Climate Change.
[5] European Commission. Directive 2008/50/EC of the European Parliament and of the Council of 21 May 2008 on ambient air quality and cleaner air for Europe. *Off J Eur Union* 2008; L152: 1-44. http://eur-lex.europa.eu/LexUriServ/LexUriServ.do?uri=OJ:L:2008:152:0001:0044:EN:PDF (2008, accessed 30 May 2017).
[6] R.M. Harrison, A.M. Jones, J. Gietl, J. Yin, D.C. Green, Estimation of the contributions of brake dust, tire wear, and resuspension to non- exhaust traffic particles derived from atmospheric measurements. Environ Sci Technol 46 (2012) 6523–6529.
[7] J. Sharaf, Exhaust Emissions and its Control Technology for an Internal Combustion Engine, Int. Jour. Engineer. Research and Appl., 3 (2013) 947-960.
[8] H. Hagino , M. Oyama, S. Sasaki, Airborne brake wear particle emission due to braking and accelerating, Wear 334-335 (2015) 44–48.

[9] COMMISSION REGULATION (EU) No 459/2012 of 29 May 2012 amending. European Union; 2012.
[10] J. Kukutschova, , V. Roubíceka, K. Malachova, Z. Pavlíckova, R. Holusab, J. Kubackova, V. Micka, D. Mac Crimmon, P. Filip, Wear mechanism in automotive brake materials, wear debris and its potential environmental impact. Wear 267 (2009) 807-817.
[11] J. Kukutschova, V. Roubicek, M. Maslan, D. Jancik, V. Slovak, K. Malachova, Z. Pavlickova, P. Filip, Wear performance and wear debris of semimetallic automotive brake materials. Wear 268 (2010) 86-93.
[12] W. Osterle, C. Prietzel, H. Kloß, A.I. Dmitriev, On the role of copper in brake friction materials. Tribol. Int. 43 (2010) 2317-2326.
[13] A. Thorpe, R.M. Harrison, Sources and properties of non-exhaust particulate matter from road traffic: a review. Sci. Total Environ. 400 (2008) 270-282.
[14] P.G. Sanders, N. Xu, T.M. Dalka, M.M. Maricq, Airborne brake wear debris: size distributions, composition, and a comparison of dynamometer and vehicle tests, Environmental Science and Technology 37 (2003) 4060–4069.
[15] J. Wahlström, Towards a Simulation Methodology for Prediction of Airborne Wear Particles from Disc Brakes. Licentiate thesis. Department of Machine Design Royal Institute of Technology, Stockholm, ISBN 978-91-7415-391-0 (2009).
[16] J. Wahlström, A Study of Airborne Wear Particles from Automotive Disc Brakes. Doctoral thesis. Department of Machine Design Royal Institute of Technology, Stockholm, ISBN 978-91-7415-871-7. (2011)
[17] J. Wahlström, L. Olander, L., U. Olofsson, Size, Shape, and Elemental Composition of Airborne Wear Particles from Disc Brake Materials, Tribol. Lett. (2010) 38:15–24
[18] S. Lawrence, R. Sokhi, K. Ravindra, H. Mao, H.D. Prain, I.D. Bull, Source apportionment of traffic emissions of particulate matter using tunnel measurements. Atmos. Environ. 77 (2013) 548-557.
[19] California State Senate Bill 346: "Hazardous materials: motor vehicle brake friction materials", http://www.leginfo.ca.gov/pub/09-10/bill/sen/sb_0301 0350/sb_346_bill_20100927_chaptered.pdf.
[20] Washington State Senate Bill 6557: "Brake Friction Material - Restriction on Use",http://apps.leg.wa.gov/documents/billdocs/2009/10/Pdf/Bills/Session%20Law%20 2010/6557-S.SL.pdf.
[21] R. Ciudin, P.C. Verma, S. Gialanella, G. Straffelini, Wear debris materials from brake systems: environmental and health issues. Sustain. City IX 2(2014) 1423-1435.
[22] M. Riediker, R.B. Devlin, T.R. Griggs, M.C. Herbst, P.A. Bromberg, R.W. Williams, W.E. Cascio, Cardiovascular effects in patrol officers are associated with fine particulate matter from brake wear and engine emissions. Part. Fibre Toxicol. 1 (2004) 2-12.
[23] J. Hur, S. Yim, M.A. Schlautman, Copper leaching from brake wear debris in standard extraction solutions. J. Environ. Monit. 5 (2003) 837-843.
[24] B. Dhir, P. Sharmila, P. Pardha Saradhi, S. Sharma, R. Kumar, D. Mehta, Heavy metal induced physiological alterations in Salvinia natans. Ecotoxicol. Environ. Saf. 74 (2011) 1678-1684.
[25] U. Olofsson, L. Olander, A. Jansson, A study of airborne wear particles generated from a sliding contact, Journal of Tribol. 131 (4) (2009) 044503
[26] G. Perricone, J. Wahlström , U. Olofsson, Towards a test stand for standardized measurements of brake emission, Proceedings of the Institution of Mechanical Engineers, Part D: Journal of Automobile Engineering 230(11) (2016) 1521-1528.
[27] G. Perricone , M. Alemani, I. Metinöz, V. Matejka, J. Wahlström, U. Olofsson, Towards the ranking of airborne particle emissions from car brakes – a system

approach, Proceedings of the Institution of Mechanical Engineers, Part D: Journal of Automobile Engineering 230 (11) (2016) 1-17.
[28] Järvinen, A., Aitomaa, M., Rostedt, A., Keskinen, J., and Yli-Ojanperä, J. (2014). Calibration of the New Electrical Low Pressure Impactor (ELPI+). J. Aerosol Sci. 69: 150–159.
[29] P.C. Verma, M. Alemani, S. Gialanella, L. Lutterotti, U. Olofsson, G. Straffelini, Wear debris from brake system materials: A multi-analytical characterization approach. Tribol. Int. 94 (2016) 249-259.
[30] L. Lutterotti, Total pattern fitting for the combined size-strain-stress-texture determination in thin film diffraction, Nuclear Inst. and Methods in Physics Research B 268 (2010) 334-340.
[31] P.C. Verma, R. Ciudin, A. Bonfanti, P.Aswath, G. Straffelini, S. Gialanella, Role of the friction layer in the high-temperature pin-on-disc study of a brake material, Wear 346-347 (2016) 56–65.
[32] K. Holmberg, P. Andersson, A. Erdemir A., Global energy consumption due to friction in passenger cars. Tribol Int. 47 (2012) 221–234.
[33] G. Straffelini, L. Maines, The relationship between wear of semimetallic friction materials and pearlitic cast iron in dry sliding, Wear 307 (2013) 75–80.
[34] D. Chan, G.W. Stachowiach, Review of automotive brake friction materials, Proc. Instn. Mech. Engrs., 218 (2004) 953-966.
[35] R.C. Dante, Handbook of Friction Materials and Their Applications, 1st ed., Woodhead Publ. (imprint of Elsevier) Cambridge, UK (2015).
[36] R.L. Cox, Engineered tribological composites. Warrendale, Pennsylvania: SAE International (2012).
[37] G.Straffelini, P.C. Verma, I. Metinoz, R. Ciudin, G. Perricone, S. Gialanella, Wear behavior of a low metallic friction material dry sliding against a cast iron disc: Role of the heat-treatment of the disc, Wear348-349(2016)10–16.
[38] P.C. Verma, L. Menapace, A. Bonfanti, R. Ciudin, S. Gialanella, G. Straffelini, Braking pad-disc system: Wear mechanisms and formation of wear fragments, Wear 322-323 (2015) 251–258
[39] A-J. Day, Braking of Road Vehicles, Butterworth-Heinemann Publ.(imprint of Elsevier) Oxford, UK (2014).
[40] F. Eddoumy, H. Kasem, H. Dhieb, J.G. Buijnsters, P. Dufrenoy, J.-P. Celis, Y. Desplanques, Role of constituents of friction materials on their sliding behavior between room temperature and 400°C, Mater. Des. 65 (2015) 179–186.
[41] F. Georges J. Sykes, Decomposition characteristics of a char-forming phenolic polymer used for ablative composites, National Aeronautics Space Administration, NASA TN D-3810, 1967.
[42] J. Bijwe, N. Majumdar, B.K. Satapathy, Influence of modified phenolic resins on the fade and recovery behavior of friction materials, Wear 259 (2005) 1068–1078.
[43] U.S. Hong, S.L. Jung, K.H. Cho, M.H. Cho, S.J. Kim, H. Jang, Wear mechanism of multiphase friction materials with different phenolic resin matrices, Wear 266 (2009) 739–744.
[44] M.H. Cho, S.J. Kim, D. Kim, H. Jang, H., Effects of ingredients on tribological characteristics of a brake lining: an experimental case study. Wear 258(2005) 1682-1687.
[45] Z. Ji, H. Jin, W. Luo, F. Cheng, Y. Chen, Y. Ren, Y. Wu, S. Hou, The effect of crystallinity of potassium titanate whisker on the tribological behavior of NAO friction materials, Tribol Int 107 (2017) 213 – 220.
[46] W. Osterle, C. Prietzel, H. Kloss, A.I. Dmitriev, On the role of copper in brake friction materials, Tribol. Int. 43 (2010) 2317-26.

[47] C. Menapace, L. Leonardi, G. Perricone, M. Bortolotti, G. Straffelini, S. Gialanella, Pin-on-disc study of brake friction materials with ball-milled nanostructured components, Materials and Design 115 (2017) 287-298.
[48] O. Nosko, U. Olofsson, Effective density of airborne wear particles from car brake materials,Journal of Aerosol Science 107 (2017) 94-106.
[49] M. Geller, S. Biswas, C. Sioutas, Determination of particle effective density in urban environments with a differential mobility analyzer and aerosol particle mass analyzer, Aerosol Science and Technology 40 (9) (2006) 709–723.
[50] W.P. Kelly, P. McMurry, Measurement of particle density by inertial classification of differential mobility analyzer-generated monodisperse aerosols, Aerosol Science and Technology 17 (3) (1992) 199–212.
[51] O. Nosko, R. Borrajo-Pelaezb, P. Hedström, U. Olofsson, Porosity and shape of airborne wear microparticles generated by the sliding contact between a low-metallic friction material and cast iron, submitted for publication (2016).
[52] N.A. Fuchs, The mechanics of aerosols, Pergamon, New York, 1964.
[53] O. Nosko, J. Vanhannen, U. Olofsson, Emissions of 1–10 nm airborne wear particles from brake materials, Aerosol Science & Techn., 51(1) (2016) 91-96.
[54] G. Straffelini, S. Verlinski, P.C. Verma, G.Valota, S.Gialanella, Wear and Contact Temperature Evolution in Pin-on-Disc Tribotesting of Low-Metallic Friction Material Sliding Against Pearlitic Cast Iron, Tribol. Letts (2016) 62 (3):36.
[55] V. Matejka; I. Metinöz, M. Alemani, J. Wahlström, A. Bonfanti, U. Oloffson, G. Perricone, Dependency of PM_{10} particles emission on stability of friction coefficient and character of friction surface, in: Eurobrake 2016 conference, 2016. Paper id: EB2016-MDS-009.
[56] I. Metinoz, V. Matejka, M. Alemani, J. Wahlström, G. Perricone , Could pin-on-disc tribometers be used to study the friction/wear performance of disc brake materials? in: Eurobrake 2016 conference, 2016. Paper id: EB2016-MDS-010.
[57] M. Alemani, O. Nosko, I. Metinoz, U. Olofsson, A Study on Emission of Airborne Wear Particles from Car Brake Friction Pairs, SAE Int. J. Mater. Manuf. 9(1) (2016)
[58] O. Nosko, M. Alemani, U. Olofsson, Temperature Effect on Emission Of Airborne Wear Particles from Car Brakes, in: Eurobrake 2015 conference, 2015. Paper id: EB2015-TEF-014
[59] M. Alemani, U. Olofsson, G. Perricone, A. Söderberg, J. Wahlström, A. Ciotti, A study on the load level influence on particulate matter emissions from the sliding contact between a low steel friction material and cast iron, in: Eurobrake 2015 conference, 2015. Paper id: EB2015-FMC-004.
[60] A. Söderberg, U. Sellgren, S. Andersson, Using finite element analysis to predict the brake pressure needed or effective rotor cleaning in disc brakes, SAE Technical Paper (2008).
[61] A. Söderberg, S. Andersson,Simulation of wear and contact pressure distribution at the pad-to-rotor interface in a disc brake using general purpose finite element analysis software Wear, 267 (2009) 2243–2251.
[62] M. Müller, G.P. Ostermeyer,A cellular automaton model to describe the three dimensional friction and wear mechanism of brake systems, Wear 263 (2007) 1175–1188.
[63] W. Österle, A. Dmitriev,Some considerations on the role of third bodies during automotive braking, SAE Int. Journ. Passeng.Cars – Mech. Syst. 7 (4) (2014) 1287–1294.
[64] J. Wahlström, A. Söderberg, U. Olofsson A cellular automaton approach to numerically simulate the contact situation in disc brakes,Tribol. Lett. 42 (2011) 253–262.
[65] M. Eriksson, J. Lord, S. Jacobson, Wear and contact conditions of brake pads: dynamical in situ studies of pads on glass,Wear 249(3-4) (2001) 272–278.

[66] G. Valota , S. De Luca, A. Söderberg, Use of FEA to Clarify Pin-On-Disc Tribometer Tests of Disc Brake Materials, in: Eurobrake 2015 conference, 2015. Paper id: EB2015-STQ-004.
[67] G. Valota , S. De Luca, A. Söderberg. Using Finite Element Analysis to Simulate the Wear in Disc Brakes During a Dyno Bench Test Cycle. Eurobrake 2017, Dredsen, Germany 2-4 May. Paper id: EB2017-SVM-003.
[68] M. Alemani, J. Wahlström , U. Olofsson, Mapping of particle emission coefficients from disc brake aerosols base on pin on disc testing, submitted for publication (2017).
[69] J . Wahlström Towards a cellular automaton to simulate friction, wear, and particle emission of disc brakes Wear, 313 (2014), pp. 75–8.
[70] J. Wahlström,A comparison of measured and simulated friction, wear, and particle emission of disc brakes. Tribology International, 92, 503-511 (2015).
[71] G. Straffelini, R. Ciudin R, A. Ciotti, S. Gialanella, Present knowledge and perspective on the role of copper in brake materials and related environmental issues: A critical assessment, Environmental Pollution 207 (2015) 211-219.
[72] LOWBRASYS:a LOW environmental impact BRAke SYStem; H2020- MG-3.1-2014_ ID PROJECT 636592-2, starting date: September 2015.